Dynamic microbial community associated with iron-arsenic co-precipitation products from a growndwater storage system in Bangladesh

UNIVERSITÀ DEGLI STUDI DI TORINO

DYNAMIC MICROBIAL COMMUNITY ASSOCIATED WITH IRON-ARSENIC CO-PRECIPITATION PRODUCTS FROM A GROUNDWATER STORAGE SYSTEM IN BANGLADESH

ROBERTA GORRA[1,2], GORDON WEBSTER[2,3], MARIA MARTIN[1], LUISELLA CELI[1], FRANCESCA MAPELLI[4], ANDREW J. WEIGHTMAN[2]

[1] DIVAPRA, University of Turin, via Leonardo da Vinci 44, 10095 Grugliasco (TO), IT

[2] Cardiff School of Biosciences, Cardiff University, Main Building, Park Place, Cardiff, Wales, CF10 3AT, UK

[3] School of Earth and Ocean Sciences, Cardiff University, Main Building, Park Place, Cardiff, Wales, CF10 3AT, UK

[4] DISTAM, University of Milan, via Celoria 2, 20133 Milano, IT

Abstract

The prokaryotic community in a Fe-As co-precipitation product from a groundwater storage tank in Bangladesh was investigated over a 5-year period to assess the diversity of the community and to infer biogeochemical mechanisms that may contribute to the formation and stabilisation of co-precipitation products and to Fe and As redox cycling. Partial 16S rRNA gene sequences from *Bacteria* and *Archaea*, functional markers (*mcrA* and *dsrB*) and iron-oxidizing *Gallionella*-related 16S rRNA gene sequences were determined using denaturing gradient gel electrophoresis (DGGE). Additionally, a bacterial 16S rRNA gene library was also constructed from one representative sample. Biogeochemical characterization demonstrated that co-precipitation products consist of a mixture of inorganic minerals, mainly hydrous ferric oxides, intimately associated with organic matter of microbial origin that contribute to the chemical and physical stabilization of a poorly ordered structure. DGGE analysis and PCR-cloning revealed that the diverse bacterial community structure in the co-precipitation product progressively stabilized with time resulting in a prevalence of methylotrophic *Betaproteobacteria*, while the archaeal community was less diverse and was dominated by members of the *Euryarchaeota*. Results show that Fe-As co-precipitation products provide a habitat characterized by anoxic/oxic niches that supports a phylogenetically and metabolically diverse group of prokaryotes involved in metal, sulphur and carbon cycling, supported by the presence of *Gallionella*-like iron-oxidizers, methanogens, methylotrophs, and sulphate-reducers. However, no phylotypes known to be directly involved in As(V) respiration or As(III) oxidation were found.

Introduction

Arsenic (As) tops the US Agency for Toxic Substances and Diseases Registry's list of dangerous elements because of its high toxicity and prevalence in the environment. According to the US Environmental Protection Agency and the World Health Organization, the maximum recommended concentration of As in drinking water is 10 μg/L, but as many as 35-40 million people in Bangladesh and West Bengal (India) are exposed to As concentrations >50 μg/L [6]. In these countries, drinking water generally derives from groundwater, in order to reduce the high incidence of waterborne diseases caused by the high microbial contamination of surface waters [59, 54].

Arsenic toxicity is determined by its speciation, which in turn is linked to redox conditions, while As mobility and concentrations in water are controlled by factors affecting adsorption/desorption and precipitation/dissolution processes, such as pH, redox potential, nature and concentration of cations, and availability of surface adsorbing sites. In natural waters, arsenate, arsenite and methylated arsenic compounds are found as the dominant As species [59]. In aerobic environments, arsenate (As(V) as $H_2AsO_4^-$ and $HAsO_4^{2-}$) is the predominant inorganic form, whereas more toxic arsenite (As(III) as H_3AsO_3 and H_2AsO_3) prevails under anoxic conditions. While arsenate mobility is limited by chemisorption to the surface of several common minerals, such as iron (Fe) and aluminium oxy(hydr)oxides, arsenite is effectively adsorbed by a fewer minerals and less strongly retained on the surfaces [59]. The strong affinity of Fe oxy(hydr)oxides towards As and the formation of Fe-As co-precipitation products have been widely studied, and the co-precipitation of Fe oxy(hydr)oxides including As and/or other contaminants is a method commonly exploited in As removal plants [26, 67].

In most As affected zones of Bangladesh, groundwater is characterized by low redox potential and high concentrations of other solutes besides As, including Fe(II) [6]. Under these conditions, the formation of Fe-As co-precipitation products following groundwater extraction is a widespread phenomenon observed whenever the water is extracted from the ground and stored in any kind of reservoir exposed to the air. This phenomenon is also traditionally exploited for natural Fe and As attenuation [57]. However, in large groundwater reservoirs, often represented by closed containers, the oxygen diffusion through the water mass could be slow, and at low oxygen concentrations the reaction rates of As(III) and Fe(II) oxidation are substantially increased by microbial processes, compared to abiotic chemical reactions [5].

Due to the natural abundance of As in the environment, many prokaryotes have adapted to detoxify or utilise high As concentrations. Representatives from several bacterial genera, such as *Bacillus*, *Escherichia*, *Staphylococcus*, *Clostridium* and *Desulfovibrio* [53] have been shown to develop resistance to As compounds, based on different plasmid or genomic *ars* gene encoded detoxification systems [46, 58]. In addition, a diverse range of other prokaryotes, including anaerobic methanogenic *Archaea* and aerobic *Bacteria* can also form methylated As compounds [53, 45]. Arsenic may also serve as an electron acceptor or donor for either dissimilatory arsenate-reducing prokaryotes or arsenite-oxidizing prokaryotes, respectively [69]. Prokaryotic populations associated with As transformations have been characterized from oxic environments [44] and anoxic freshwater sediments naturally contaminated with As [18, 68, 14].

Arsenic mobility is influenced by co-precipitation or adsorption on minerals such as Fe oxy(hydr)oxides and consequently iron-associated bacteria may indirectly affect As water concentrations. Under microaerophilic conditions, aerobic Fe(II) oxidizers form Fe minerals that may bind As and co-precipitate [33, 9], whereas anaerobic Fe(II) oxidizers are the most important catalysts for the generation of Fe biogenic minerals under anoxic conditions [62]. Prokaryotic Fe and As oxidations also promote and stabilize co-precipitation resulting in scavenging of As from water, archaeal and bacterial reducing metabolisms using labile organic matter may induce As release [54]. The concentration of As in drinking water is further affected by the interaction of microorganisms with minerals that may change surface properties and modify the solid/solution partition of the element.

The main objective of this study was to determine the prokaryotic community composition of Fe-As co-precipitation products formed naturally in a groundwater storage tank located in an arsenic contaminated area in South-West Bangladesh. Samples of Fe-As co-precipitation products were taken over a period of five years and analysed by bacterial and archaeal 16S rRNA gene PCR-DGGE and PCR-cloning to identify dominant prokaryotes, and evaluate prevalent microbial and chemical mechanisms controlling As speciation and cycling during groundwater storage.

Methods

Site characteristics

The study area is located in South-West Bangladesh, Khulna Division, Satkhira District (22°44’39.4"N; 89°05’44.8"E), where groundwater As levels are in the range 100-200 μg/L. A 2000-litre volume black plastic groundwater storage tank located on the upper floor of a

hospital building, to supply water to several bathrooms, typical for the area, was chosen for this study. The tank was filled directly from a groundwater tube well by an electric pump, automatically activated by the lowering of the water level (1 m). Hence, a minimum of nearly 1 m water and layer of about 10-15 cm of co-precipitation product were always present in the tank.

Water sampling and chemical characterisation

Water samples were collected from the inlet pipe into the reservoir tank annually between 2005 and 2009. A series of sub-samples were immediately acidified with concentrated HCl to avoid precipitation, and another series were untreated and stored in completely filled polyethylene bottles. Untreated water samples were analysed potentiometrically for pH with a pH meter (model micro pH-2001, Crison Instruments) and for electrical conductivity with a conductometer (micro CM 2201, Crison Instruments) with a platinum electrode. The major dissolved cations and arsenic species were determined in the acidified subsamples by ICP-AES (IRIS II Advantage, Thermo Jarrell Ash), while chloride, sulphate and nitrate were determined on untreated subsamples by ion chromatography (Dionex DX 50, 2 mm system, AS9 analytical column with AG9 guard column, eluent: 9 mM sodium carbonate, flux rate: 0.25 ml min^{-1}). Dissolved phosphorus and ammonium were determined colorimetrically [51] on the acidified subsamples, and dissolved organic carbon (DOC) and total dissolved nitrogen (TdN) were determined with a TOC analyser (Elementar Vario TOC cube).

Co-precipitation product sampling and chemical characterization

Iron-As co-precipitation products were also sampled from the groundwater storage tank during the same period, and transferred in acid-washed polyethylene bottles, completely filled without head space. After cold shipping to the laboratory, co-precipitation product sub-samples were stored at 4°C for chemical characterization, and 2 or 3 replicate co-precipitate samples were stored at -20ºC for DNA extractions.

The co-precipitation products were characterised for the elemental composition after *aqua regia* digestion (nitric acid and hydrochloric acid a volume ratio of 1:3) of the freeze-dried samples, and determination of the major inorganic components by ICP-AES. Arsenic was determined with the same instrument after hydride generation. The total nitrogen, organic and inorganic carbon concentrations were determined with a Carlo Erba NA Protein 2100 elemental analyzer, with or without removal of the inorganic carbon with HCl treatment of the freeze-dried sample.

The organic fraction present in the co-precipitation products was separated by extraction from the fresh samples with 0.5 M HCl/0.3 M HF to solubilise iron and silica precipitates. The inorganic constituents were easily solubilised and a colourless, mucilaginous material was separated by centrifugation at 1600 x *g,* washed with deionised water several times, until *ca.* pH 2, and then freeze-dried. The ash content was below 2%. The organic fraction was characterised using FT-IR and ^{13}C-NMR spectroscopy. The FT-IR spectra were recorded on a Perkin Elmer 16F PC FT-IR spectrophotometer; the pellets were prepared by pressing under vacuum 1 mg of organic material with 400 mg of KBr (spectrometry grade) and spectra acquired at 4 cm^{-1} resolution and 64 scans were averaged. Liquid-state ^{13}C-NMR spectra were recorded at 50.3 MHz on a Varian Gemini 200 spectrometer by dissolving 100 mg of each sample in 1 mL of 0.5 M NaOD. The spectra were obtained using inverse-gated decoupling with an acquisition time of 0.2 s, a 45° pulse angle and relaxation time of 2 s; total acquisition time was 24 h [12]. The free induction decays were processed by applying 50 Hz line broadening and baseline correction. In order to estimate the carbon composition of the organic fraction quantitatively, the ^{13}C-NMR spectra were divided and integrated across the following ranges: 0-50, 50-65, 65-105, 105-160 and 160-185 ppm.

Scanning electron microscopic analysis

Co-precipitation product samples for SEM were fixed at 4ºC for 12 h with 2.5% glutaraldehyde, dehydrated with a series of ethanol baths (50-100% vol/vol) and chemically dried with hexamethyldisilazane [3]. Samples were coated with gold using a sputtering diode and observed under a Cambridge S-360 SEM.

DNA extraction

Total DNA was extracted from co-precipitation products using a modified DNA isolation procedure described by Zhou et al. [76]. Essentially, DNA was extracted from 0.6 g of frozen material by mechanical disruption with 1 g sterilised (after 170^{o}C for 4 h) zirconia-silica beads in a sodium phosphate-buffered SDS solution [25] using a FastPrep 24 instrument (MP Biomedicals). The DNA pellet was re-suspended in 50 μL of sterile DNase treated water (Sigma) and the quantity and quality of extracted DNA was evaluated using a NanoDrop ND-1000 spectrophotometer (Nanodrop Technologies) and agarose gel electrophoresis. Quantified DNA was stored at -80ºC until required for molecular analysis.

PCR conditions

PCR amplifications were performed in a DNA Engine Dyad Thermal Cycler gradient block (MJ Research). For PCR-DGGE, total bacterial 16S rRNA genes were amplified directly from the co-precipitation product DNA, while *Archaea*, methanogen and *Gallionella*-like iron-oxidizing bacteria 16S rRNA genes, *dsrB* (dissimilatory sulphite reductase) and *mcrA* (methyl-coenzyme M reductase) genes were amplified by a nested PCR approach (Table 1). All PCR primers used in this study are listed in Table 1 and reaction conditions were as previously described [4, 18, 69, 72, 70]. The PCR mixtures were contained in a total volume of 50 μL, 0.4 pmol μL^{-1} of primers (Eurofins MWG Operon), 1 μL of co-precipitation product DNA template, 1 x reaction buffer (Bioline), 1.5 mM $MgCl_2$, 1.5 U Biotaq DNA polymerase (Bioline), 0.25 mM each dNTP (Promega Corporation), 10 μg bovine serum albumin (BSA; Promega Corporation). The reaction mixtures for PCR of *dsrB* and *mcrA* were as above, except 2.5 mM $MgCl_2$ was added. All second rounds of nested PCR were all performed without BSA.

DGGE analysis

Denaturing gradient gel electrophoresis (DGGE) was carried out as previously described [72] using a DCode™ Universal Mutation Detection System (Bio-Rad Laboratories) with a gradient between 30 and 60%. Electrophoresis was at 200 V for 5 h (with an initial 10 min at 80 V) at 60°C in 1 × TAE buffer. DGGE gels were stained with SYBR Gold nucleic acid gel stain (Invitrogen) for 30 min and viewed under UV. Gel images were captured with a Gene Genius Bio Imaging System (Syngene). All *mcrA* genes were amplified without a GC clamp and analysed on 25-50% denaturant gradient gels [73]. DGGE bands of interest were excised, re-amplified by PCR, sequenced as described previously [71, 55] and searched for sequence similarities in the NCBI database using nucleotide BLAST analysis [1]. DGGE profiles were analysed as described [74] using the software Community Analysis Package version 3.1 (Pisces Conservation Ltd). It should be noted that initial DGGE analysis of bacterial 16S rRNA genes from replicate samples of Fe-As co-precipitation products for each sample year produced identical *Bacteria* and *Gallionella*-like 16S rRNA gene DGGE profiles and therefore all subsequent PCR-DGGE analysis (*Bacteria*, *Archaea* and specific functional groups) were undertaken on one representative sample per year.

Bacterial 16S rRNA gene library and phylogenetic analysis

DNA from the co-precipitation product sampled in 2008, chosen on the basis of PCR-DGGE screening, was used to construct a bacterial 16S rRNA gene library. Bacterial primers 27F and 1492R [37] were used to amplify almost the complete 16S rRNA gene using the following amplification program: 94°C (5 min), 5 cycles of 94°C (1 min), 50°C (1 min), 72°C (2 min), followed by 30 cycles of 94°C (1 min), 55°C (1 min), 72°C (2 min), completed with an additional 10 min at 72°C. Replicate amplification products were purified with the QIAquick PCR Purification Kit (Qiagen), pooled and ligated into the linear Plasmid Vector pCR4 supplied with the TOPO TA CloningR Kit for Sequencing (Invitrogen) and subsequently transformed into One Shot Chemically Competent *Escherichia coli* (Invitrogen) by heat shock following the manufacturer's protocol. Positive transformants were screened for correct size of the insert by direct PCR using primers M13F and M13R and plasmid inserts were sequenced using M13F primer by Macrogen (http://www.macrogen.co.kr).

Sequence chromatographs were analyzed using the Chromas Lite software package version 2.01 (http://www.technelysium.com.au/). Sequences were checked for chimeras with Bellerophon software [29] and searched for sequence similarities in databases using nucleotide BLAST analysis [1]. All nucleotide sequences were aligned using ClustalX [66] with sequences retrieved from the database. Alignments were edited manually using BioEdit Sequence Alignment Editor version 7.0.9.0 [21] and regions of ambiguous alignment were removed. The phylogenetic relationships between pairs of 16S rRNA gene sequences were determined using distance and implemented in MEGA4 [65]. The LogDet distance analysis [42] constructed using minimum evolution was used as the primary tool for estimating phylogenetic relationships, but other methods including p-distance and Jukes–Cantor with minimum evolution and neighbour-joining were also carried out, which yielded similar tree topologies. All distance trees were bootstrapped 1000 times to assess support for nodes.

All 16S rRNA, *mcrA* and *dsrB* gene sequences retrieved during this study were deposited in the EMBL database (http://www.ebi.ac.uk/embl/) under accession numbers HE577673 to HE577789.

Results

Water chemical characteristics

The mean water pH was 7.2 and electrical conductivity 840 µS cm^{-1}, reflecting the presence of dissolved electrolytes (Table 2). The major dissolved cations were Ca^{2+}, Na^{+}, Mg^{2+}, Si^{4+} and Fe^{2+} with lower amounts of trace elements. Dissolved anions were mainly represented by chloride (55 mg/L) and phosphorus, with a relatively low concentration of sulphate (~1 mg/L). The average arsenic concentration was 64.7 µg/L with very little change during the 2005 to 2009 sampling period. Dissolved organic carbon (8.82 mg/L) and TdN (5.31 mg/L) were in the higher ranges reported in studies performed in different parts of Bangladesh [24]. Nitrogen was mainly in the form of dissolved ammonium (3.61 mg/L) and/or bound to soluble organic molecules, as suggested by the difference between TdN and ammonium concentrations, while neither nitrate nor nitrite anions were detected. Overall, during the study period the range and quantity of solutes in the analysed waters remained relatively constant.

Co-precipitation product characteristics

The chemical composition of the co-precipitation products (Table 3) reflected that of the incoming water, although different proportions of most elements were detected. The solid mainly consisted of iron (37% of the total dry mass), probably in the form of poorly ordered oxides and hydroxides [57]. Calcium (6.0%) and phosphorus (2.7%) were the most abundant other elements, and arsenic constituted *ca.* 0.23% of the co-precipitation product. Considerable amounts of barium, zinc, magnesium were also detected, together with lower concentrations of potassium, sodium, manganese and copper. Carbon represented on average 4.7% of the total mass, most of which was in organic form; total nitrogen was 0.39% and sulphur around 0.02%.

The FT-IR spectrum of the organic material (Figure 1A) showed the presence of an aliphatic fraction, suggested by bands centred at 2920 and 2850 cm^{-1} (-CH_3 and –CH_2- stretching, respectively) and by a band at 1450 cm^{-1} (-CH_2- and -CH_3 bending). The band at 1650 could be attributed to C=C stretching of aromatic rings, while the prominent peak at 1538 cm^{-1} (N-H bending of amide II groups) suggests presence of proteinaceous residues. In contrast the weak shoulder at 1720 cm^{-1}, together with the small peak at nearly 1200 cm^{-1} indicates a low presence of C=O groups. The asymmetric C-O stretching and the C-OH bending of tertiary alcohols at 1236 cm^{-1}, together with the peak at 1150 cm^{-1} and the broad band at 1050-1020 cm^{-1} suggest a large presence of saccharidic material.

Figure 1B shows the liquid state ^{13}C-NMR spectrum of the extracted organic material, suggesting an important contribution of alkyl C with signals at 16, 29 and 31 ppm, accounting for 44.1% of C. The signals at 57 ppm are attributed to C-N carbons of proteinaceous residues and to O-CH_3 C (7.8%), while the 63-105 ppm region is characteristic of saccharidic C. However, the proportion of the aromatic C was low (13.9%), and similarly that of phenolic-OH groups, suggesting the absence of lignin-derived phenols. Conversely, the 165-185 ppm pattern attributed to C=O C of carboxyl and amide groups was more intense, and split into various signals, with higher intensity for those at lower chemical shift. The interpretation of the FT-IR and ^{13}C NMR spectra is based on data reported in Celi *et al*. [11], and references therein.

Scanning electron microscopy

The SEM examination of the co-precipitation product (Figure 2) revealed the presence of poorly-ordered metal oxides crossed by distinct helical bacterial structures that resemble the stalks of *Gallionella ferruginea* [35]. Scanning electron micrographs show that these prokaryotes are diffused in the co-precipitation product and have granular structures on their surface (Figure 2B), which may represent ferric iron deposits. Previous investigations of *Gallionella* species have demonstrated that stalks of these bacteria typically become encrusted with poorly ordered iron oxide precipitates [34, 35]. SEM analysis showed that stalks were the prevalent prokaryotic structures, although some cocci-like structures were also observed (data not shown). However, the absence of other obvious prokaryotic forms in SEM pictures may be ascribed to the preparation procedures potentially altering the architecture and composition of samples.

Prokaryotic community in the Fe-As co-precipitation products

Bacterial and archaeal community structures of the Fe-As co-precipitation products sampled from the bottom of the water tank during 2005 and 2009 were determined by 16S rRNA gene PCR-DGGE and PCR-cloning. Initial PCR-DGGE analysis on replicate samples of the Fe-As co-precipitate (data not shown) demonstrated that the prokaryotic community was homogenous throughout the 10-15 cm co-precipitate layer at the bottom of the tank and therefore further analysis was only undertaken on one representative sample per year.

Bacterial community structure assessed by PCR-DGGE

Bacterial DGGE profiles for each co-precipitation product sample were relatively complex (average of 20 bands), and often dominated by 2 to 6 brightly stained bands and several other less intense bands (Figure 3A). Analysis of excised and sequenced DGGE bands demonstrated at least 15 different bacterial phylotypes belonging to four different phyla (*Proteobacteria, Chloroflexi, Nitrospirae* and candidate division SR1), as well as other unclassified bacteria related to novel sequences found in suboxic sediments or contaminated soils (Table 4), suggesting a diverse bacterial population. Interestingly, many of the bacterial phylotypes detected were related to known bacterial genera (91-100% sequence similarity; Table 4) and some were very closely related to described bacterial species (>97% sequence similarity).

Cluster analysis of the bacterial DGGE profiles revealed a clear change in the bacterial community during the 5-year (2005 to 2009) study period after 2007 (Supplementary figure S1) with a succession in the dominant phylotypes (Figure 3A; Table 4). Samples from 2005-2006 were dominated by *Nitrospirae, Alphaproteobacteria* and unclassified bacteria, while during the years 2007-2009 co-precipitation products became dominated by phylotypes affiliated to the *Betaproteobacteria,* including bacteria belonging to (96-99% sequence similarity) *Methylovorous, Gallionella and Hydrogenophaga* species. In addition, the DGGE analysis also suggests a progressive stabilization of the bacterial population with time, as very similar DGGE band profiles were obtained for the last two years. Some bacterial phylotypes were present throughout the whole of the sampling period and these sequences (e.g. DGGE bands B1, B11 and B21) were related to novel bacteria from the candidate division SR1 and members of the genera *Hyphomicrobium* and *Methylocystis* (*Alphaproteobacteria*).

Bacterial 16S rRNA gene library

Based on DGGE results, the sample of 2008 was selected to construct a bacterial 16S rRNA gene library of the stabilised co-precipitation product community in order to obtain more phylogenetic resolution and sample coverage. Ninety-six clones containing plasmid inserts were originally chosen at random and sequenced. Sequences were analysed for sequence quality and after exclusion of poor quality sequences and chimeras, 70 clones were further analysed. Phylogenetic analysis indicated that the 16S rRNA gene sequences representing species of the *Proteobacteria*, *Nitrospirae*, *Bacteroidetes*, *Verrucomicrobia*, *Chlorobi*, *Chloroflexi*, *Acidobacteria*, candidate divisions OP11/OD1/SR1 and other unclassified bacteria, largely in agreement with major taxa identified by bacterial PCR-DGGE (Figure

3A; Table 4). The most abundant phylotypes were found to be within the *Proteobacteria* (Figure 4), accounting for 63% of the gene library, with *Betaproteobacteria* having the highest number of representative clones (35 clones) within this phylum. A large number of proteobacterial sequences were closely related to methyl-/methanotrophic bacteria within the *Beta*- and *Gammaproteobacteria* (Figure 5), assigned to the orders *Methylophilales* and *Methylococcales*, respectively. Other proteobacterial sequences were closely related to members of the metabolically diverse *Burkholderiales*, and novel sequences from the *Betaproteobacteria*, as well as some sequences assigned to *Deltaproteobacteria* previously reported to be present in iron-rich environments and anaerobic reactors (Figure 5).

The second most dominant group of bacteria (17%; Figure 4) belonged to members of the "former" candidate division OP11 [30], which has now been split into three distinct division level clades: SR1 (Sulfur River 1), OD1 (OP11-derived 1) and the "revised" OP11 divisions [23]. The OP11/OD1/SR1 group constitutes one of the most widely distributed candidate divisions in environmental surveys and has been retrieved from a variety of anoxic and suboxic habitats [7, 23].

Despite the detection of structures morphologically analogous to *Gallionella* stalks with SEM (Figure 2) and light microscopy (data not shown), and the high similarity to *Gallionella*-like bacteria detected by PCR-DGGE (Figure 3A; Table 4), no *Gallionella* sequences were found in the bacterial 16S rRNA gene library. This observation may be explained by the different biases of the two sets of bacterial 16S rRNA gene primers used for PCR-cloning and PCR-DGGE [28]. For example, Li et al. [39] demonstrated that *Gallionella* was preferentially amplified by using primers targeting V1-V3 and V3-V5 hypervariable regions with respect to V8, and subsequent analysis of primer 1492R using the RDP PROBE MATCH software (http://rdp.cme.msu.edu/) demonstrated that it only matched 14% (13 hits out of 92 relevant 16S rRNA gene sequences with complete 3' end) of the *Betaproteobacteria* order *Nitrosomonadales* database sequences. However, it should be noted that only a relatively low number of published 16S rRNA gene sequences have complete data at the 3' end.

Archaeal community structure assessed by PCR-DGGE

Although the archaeal community within the co-precipitation products was much less diverse than the bacterial community (Figure 3B), distinct changes in the archaeal DGGE profiles were observed, in line with those seen in the bacterial profiles, once again indicating a succession of the dominant phylotypes (Supplementary Figure S2). The 2007-2009 profiles

were relatively stable and dominated by members of the *Euryarchaeota,* related to sequences previously found in an iron-rich microbial mat (Table 5). However, prior to this stabilisation the archaeal community was initially dominated by methanogen-related sequences in 2005 and novel *Crenarchaeota* in 2006.

Specific prokaryotic functional groups

Since PCR-DGGE and PCR-cloning gave different results regarding the detection of *Gallionella*, specific *Gallionella*-targeted primers [70] were used to confirm the presence and diversity of *Gallionella*-like bacteria in Fe-As co-precipitation product samples over the sampling period (Figure 6A). *Gallionella*-specific 16S rRNA gene DGGE analysis clearly demonstrated that *Gallionella* were present in all co-precipitation products with the exception of sample 2005. All bands obtained were excised and sequenced, and were assigned to the same bacterial phylotype, with a high sequence similarity (99 to 100%, Table 5) to a *Gallionella*-like sequence previously retrieved from an iron-rich wetland soil [70]. In addition, the sequences retrieved by *Gallionella*-specific PCR-DGGE were also related (96% sequence similarity) to the *Gallionella*-like sequence (band B10) identified by bacterial PCR-DGGE (Figure 3A; Table 4).

To demonstrate that anoxic conditions/niches suitable for prokaryotes with reducing metabolisms can also exist within the Fe-As co-precipitation product, specific PCR-DGGE approaches were used to target terminal-oxidising *Bacteria* and *Archaea*. Methanogenic *Archaea* were detected in Fe-As co-precipitation product samples using both specific 16S rRNA (*Methanosarcinales* and *Methanomicrobiales*; Figure 6B; Table 5), while sulphate-reducing bacteria were targeted using *dsrB* gene primers (Figure 6C; Table 5). PCR-DGGE analysis showed that during the sample period the specific methanogen population stabilised with time and was dominated by novel sequences belonging to the *Methanomicrobiales,* similar (94% sequence similarity) to sequences previously found in acidic peatlands [10]. By contrast, the sulphate-reducing bacterial population remained almost constant throughout the study period, and novel *dsrB* sequences were distantly related (80-83% sequence similarity) to sequences from *Desulfarculus baarsii* and clones retrieved from polluted groundwaters [75]. The presence of methanogenic *Archaea* were further confirmed in samples from year 2008 and 2009 by the detection of *mcrA* genes (Table 5) belonging to unidentified methanogen *mcrA* clusters previously found in rice field soils [13] and acidic peatland bog [61].

Discussion

The primary aim of this work was to investigate the prokaryotic community in a Fe-As co-precipitation products from a groundwater storage tank during a 5-year period to identify and elucidate the stability of the population and to obtain an indication of the prevalent biotic mechanisms that may contribute to Fe and As redox cycling and subsequent soluble As levels in drinking waters. The chemical composition of the groundwater sampled was relatively stable during the study period (2005-2009), with standard deviations well within 10% for most inorganic elements, including As. Arsenic concentrations were higher than the maximum recommended concentration of As in drinking water (10 μg/L), and were in the highest frequency class (50-200 μg/L) reported for the wells of Satkhira district [6], posing a serious threat to human health.

Variability in concentrations with time were observed in TdN and DOC with values in the higher range of those reported previously in studies from different areas of Bangladesh [24]. In our study the high concentrations of TdN were mainly represented by ammonium N, since oxidised N forms were not detected indicating anoxic conditions within the water tank. Positive correlations between DOC and As water profiles have previously been found in ponds and surface waterbodies [24, 49]; therefore, the high DOC content observed in the present study may favour As release to groundwater.

Such high concentration of Fe, As and other dissolved compounds within the groundwater would determine the formation and composition of the co-precipitation products in the tank. Here we report that the co-precipitation products were represented by complex mixtures of inorganic precipitates, mainly hydrous ferric oxides, intimately mixed with organic matter. Chemical equilibrium models and experimental data suggested the precipitation of hydrous Fe oxides together with As and P, and the formation of Fe-O-P and Fe-O-As bonds prevented the transformation into crystalline Fe oxides [67]. In addition, important amounts of organic matter dominated by proteinaceous residues were present in the co-precipitation product. Carbohydrate structures were also present at higher concentrations than usually found in soils and sediments [36], while aromatic carbon groups (lignin derived compounds) were almost absent. This chemical signature suggests that the organic material co-precipitated with the mineral components is of prokaryotic origin with little contribution of plant derived compounds. Furthermore, the organic material showed a low degree of decomposition, as the 1720 cm^{-1} band signifying carboxyl groups in the FT-IR spectrum was virtually absent, and the signals in the 165-185 ppm region (^{13}C-NMR) were due to amide groups rather than carboxyls, suggesting a viable prokaryotic population. The low degree of

decomposition and type of material does suggest that microorganisms have developed through the formation of a polysaccharidic biofilm tightly linked to the Fe-mineral phase enhancing both prokaryotic biochemical activity and physico-chemical protection of the organic matter [32]. In turn, this organic component would also contribute to the physical stabilisation of the poorly ordered structure of the co-precipitation product, resulting in the long-term preservation of a highly active surface area and As retention capacity [68].

The presence of a sustained microbial population within the co-precipitation products is supported by the water chemical composition. In particular, the high concentrations of DOC and other essential elements could represent a potential source of nutrients for microbial communities even after water withdrawal, although it would be expected that the As-rich environment and the limited oxygen availability through the water volume could reduce microbial metabolic potential [24, 27, 49]. Therefore, the water storage system studied here presents the chemical and biological potential for the development of a wide range of microbial metabolisms.

PCR-DGGE analysis revealed that from 2005 to 2009 there was a distinct change in the bacterial community structure with a succession in the dominant taxa from *Alphaproteobacteria* and *Nitrospirae* in 2005 and 2006 to *Betaproteobacteria* from 2007 to 2009. The relevance of *Betaproteobacteria* in the co-precipitation product in the last years was confirmed by clone library analysis of 2008 sampling. This is in accordance with others who have reported a predominance of *Proteobacteria* in arsenic contaminated groundwaters [64], shallow waters [17] and sediments [38].

The consistent presence of *Gallionella*-like bacteria in the co-precipitate throughout the sampling period highlights the organism's potential role in As cycling by increasing the chemical stability of co-precipitation products and As immobilization. The role and effectiveness of *Gallionella* in As removal from water by producing biogenic iron oxides and potentially oxidizing As (III) has been demonstrated in several studies. For example, Katsoyannis and Zouboulis [34] showed simultaneous removal of As during Fe oxidation by *Gallionella ferruginea*, while Battaglia-Brunet et al. [5] determined the influence of As(III) and Fe(II) oxidizers on As removal from contaminated waters. Bruneel et al. [9] demonstrated the involvement of *Gallionella ferruginea* in As natural remediation process in waters from mine tailings, and Ohnuky et al. [52] reported that a *Gallionella* sp. was the predominant microorganism in a microhabitat from discharged mine waters contaminated by As.

Gallionella may successfully compete for Fe (II) and As (III) oxidation with chemical reactions due to the circumneutral conditions of this system [16, 48], and the low oxygen availability Battaglia-Brunet et al. [5]. Microaerophilic Fe(II)-oxidizing *Gallionella* species are neutrophilic and develop at the interface between oxic and anoxic environments, because of the short half-life of soluble Fe(II) in aerobic circumneutral environments [60, 22]. For these reasons *Gallionella* have been considered as indicators of steep oxygen gradients in sediments, contributing by scavenging oxygen and allowing anaerobic bacteria to exist closer to the zone of Fe(II) microbial oxidation [60]. Thus in the co-precipitation products studied here, the constant presence of *Gallionella*-like bacteria may successfully oxidize Fe (II) and As (III), and promote steep oxygen gradients. The presence of oxic/anoxic niches was confirmed by the DNA-based analysis of the associated microbial community, which showed the presence of both obligate aerobes and anaerobes.

Activity of iron-oxidizing bacteria increased the stability of the iron arsenic co-precipitation product, promoting the formation of biogenic iron oxides and, potentially, arsenite oxidation. Conversely, the release of As and Fe from the co-precipitation product into water depended on anaerobic prokaryotes. Candidate divisions SR1 and OD1, both formerly belonging to the OP11 candidate division, were a significant component of the co-precipitation product community (i.e. 17% of the clones; Figure 4) throughout the sampling period (Figure 3; Table 4). *Bacteria* belonging to these candidate divisions have been retrieved in many anoxic and suboxic iron- and sulphur-rich environments, and Borrel et al. [7], investigating the potential ecological role of SR1 and OP11 members, postulated that some members might be involved in dissimilatory Fe(III) reduction. This may also be the case in the co-precipitation product studied here, in which these bacteria could occupy anoxic niches or zones within the precipitates. Despite the wide distribution of SR1, OD1 and OP11 candidate divisions, including their detection in contaminated sediments, this is the first time that they have been detected in As-rich environments.

Deltaproteobacteria were not detected with bacterial PCR-DGGE but represented 3% of the 16S rRNA gene library, and could promote co-precipitation product solubilisation. Islam et al. [31] demonstrated that *Deltaproteobacteria* could play a role in Fe and As reduction and release of these elements from sediments, but this capacity is severely limited by the availability of electron donors. The consistent presence of methanogens and sulphate reducers alongside aerobic bacteria further confirms the intimate association of aerobic and anaerobic micro-niches in this system. Methanogenic *Archaea* and sulphate reducers play an important role in As-methylation, causing As loss by volatilization. Furthermore, Liu et al.

[41] demonstrated that the methanogen *Methanosarcina barkeri* is able to reduce iron oxides. Thus the presence of methanogens and sulphate-reducers may compromise the stability of the co-precipitation products and release As and Fe. On the other hand, the high percentage of aerobic methylophilic/methanotrophic bacteria, which is in agreement with other investigations on As-contaminated mine-drainage water, groundwater and sediments [5, 27, 63], and their ability to consume a wide range of C_1 compounds, such as methane, methanol, and methylated sulfur species [2, 40], could indicate a metabolic advantage of such bacteria to develop in As-rich environments, possibly due to their capacity to utilize methylated arsenic compounds.

Conclusions

The groundwater filling the storage tank system studied here contained high concentrations of As, Fe and dissolved organic compounds. The formation of a large amount of microbial organic material, intimately bound to the mineral matrix, appears to determine a physical and chemical stabilisation of the co-precipitation products and, hence, reduces the amount of As present in the water. The chemical environment with circumneutral conditions and low availability of oxygen was suitable for a relatively wide range of microbial metabolisms which more likely prevailed for As and Fe redox reactions over the chemical processes. Although the metabolic capabilities of phylotypes cannot be directly determined from the phylogenetic relationship to cultured species, our results suggest that co-precipitation products provide a habitat for a phylogenetically and metabolically diverse group of prokaryotes involved in metal, sulphur and carbon cycling, supported by the presence of *Gallionella*-like iron-oxidizers, methanogens, methylotrophs, and sulphate-reducers. We propose that these prokaryotes indirectly drive the fate of As within the system. However, surprisingly, no phylotypes known to be directly involved in As(V) respiration or As(III) oxidation were found.

The microbiology of the Fe-As co-precipitation products was consistent with observations that Fe(II)-oxidizing bacteria are important in the development and stability of iron oxides. In addition, results suggest the co-existence of oxic and anoxic environments which may also promote Fe and As reduction and therefore mobilization of As into the water and/or volatilization as methylated compounds. The equilibrium among the several microbial metabolisms potentially present in the As-contaminated water and associated co-precipitate could be a key factor contributing to the control of As chemical speciation and solid/liquid partitioning in groundwater reservoirs, and therefore, human exposure. Further investigations

should aim to evaluate if methylophilic bacteria identified in this system have a direct role in the evolution of As species.

Aknowledgements

The authors would like to thank Dr. Emanuele Costa and Dr Linda Pastero. (Dipartimento di Scienze Mineralogiche e Petrologiche, Universita degli Studi di Torino) for their support in Scanning Electron Microscopy and HG-ICP-AES analysis respectively. This work was supported by the Italian Research Program of National Interest (PRIN 2008) for the financial support of the research. Rishilpi Development Project Bangladesh and Ms. R. Ferdousi are gratefully acknowledged for the logistic support.

References

1. Altschul SF, Gish W, Miller W, Myers EW, Lipman DJ (1990) Basic Local Alignment Search Tool. J Mol Biol 215: 403-410
2. Anthony C (1982) The biochemistry of methylotrophs. Academic Press, New York
3. Araujo JC, Teran FC, Oliveira RA, Nour EAA, Montenegro MAP, Campos JR, Vazoller RF (2003) Comparison of hexamethyidisilazane and critical point drying treatments for SEM analysis of anaerobic biofilms and granular sludge. J Electron Microsc 52: 429-433
4. Banning N, Brock F, Fry JC, Parkes RJ, Hornibrook ERC, Weightman AJ (2005) Investigation of the methanogen population structure and activity in a brackish lake sediment. Environmental Microbiology 7: 947-960
5. Battaglia-Brunet F, Itard Y, Garrido F, Delorme F, Crouzet C, Greffie C, Joulian C (2006) A simple biogeochemical process removing arsenic from a mine drainage water. Geomicrobiol J 23: 201-211
6. BGS, DPHE (2001) Arsenic contamination of groundwater in Bangladesh. In: Kinniburgh, DG, Smedley, P.L. (ed.) British Geological Survey (Technical Report, WC/00/19). British Geological Survey, Keyworth
7. Borrel G, Lehours AC, Bardot C, Bailly X, Fonty G (2010) Members of candidate divisions OP11, OD1 and SR1 are widespread along the water column of the meromictic Lake Pavin (France). Arch Microbiol 192: 559-567
8. Brosius J, Dull TJ, Sleeter DD, Noller HF (1981) Gene organization and primary structure of a ribosomal RNA operon from Escherichia coli. J Mol Biol 148: 107-127

9. Bruneel O, Duran R, Casiot C, Elbaz-Poulichet F, Personne JC (2006) Diversity of microorganisms in Fe-As-Rich acid mine drainage waters of Carnoules, France. Appl Environ Microbiol 72: 551-556
10. Cadillo-Quiroz H, Brauer S, Yashiro E, Sun C, Yavitt J, Zinder S (2006) Vertical profiles of methanogenesis and methanogens in two contrasting acidic peatlands in central New York State, USA. Environmental Microbiology 8: 1428-1440
11. Celi L, Schnitzer M, Negre M (1997) Analysis of carboxyl groups in soil humic acids by a wet chemical method, Fourier-transform infrared spectrophotometry, and solution-state carbon-13 nuclear magnetic resonance. A comparative study. Soil Science 162: 189-197
12. Cerli C, Celi L, Kaiser K, Guggenberger G, Johansson MB, Cignetti A, Zanini E (2008) Changes in humic substances along an age sequence of Norway spruce stands planted on former agricultural land. Organic Geochemistry 39: 1269-1280
13. Conrad R, Klose M, Noll M, Kemnitz D, Bodelier PLE (2008) Soil type links microbial colonization of rice roots to methane emission. Global Change Biology 14: 657-669
14. Cummings DE, Caccavo F, Fendorf S, Rosenzweig RF (1999) Arsenic mobilization by the dissimilatory Fe(III)-reducing bacterium Shewanella alga BrY. Environmental Science & Technology 33: 723-729
15. Delong EF (1992) Archaea in coastal marine environments. Proceedings of the National Academy of Sciences of the United States of America 89: 5685-5689
16. Emerson D, Revsbech NP (1994) Investigation of an iron-oxidizing microbial mat community located near Aarhus, Denmark - Laboratory studies. Appl Environ Microbiol 60: 4032-4038
17. Gault AG, Islam FS, Polya DA, Charnock JM, Boothman C, Chatterjee D, Lloyd JR (2005) Microcosm depth profiles of arsenic release in a shallow aquifer, West Bengal. Mineral Mag 69: 855-863
18. Geets J, Borrernans B, Diels L, Springael D, Vangronsveld J, van der Lelie D, Vanbroekhoven K (2006) DsrB gene-based DGGE for community and diversity surveys of sulfate-reducing bacteria. Journal of Microbiological Methods 66: 194-205
19. Grosskopf R, Stubner S, Liesack W (1998) Novel euryarchaeotal lineages detected on rice roots and in the anoxic bulk soil of flooded rice microcosms. Appl Environ Microbiol 64: 4983-4989

20. Hales BA, Edwards C, Ritchie DA, Hall G, Pickup RW, Saunders JR (1996) Isolation and identification of methanogen-specific DNA from blanket bog feat by PCR amplification and sequence analysis. Appl Environ Microbiol 62: 668-675
21. Hall TA (1999) BioEdit: a user-friendly biological sequence alignment editor and analysis program for Windows 95/98/NT. Nucleic Acids Symposium series 41: 95-98
22. Hanert HH (2006) The genus *Gallionella*. In: Dworkin, M, Falkow, S, Rosenberg, E, Schleifer, KH, Stackebrandt, E (eds.) The Prokaryotes, vol. 7. Springer-Verlag, New York, USA, pp. 990-995
23. Harris JK, Kelley ST, Pace NR (2004) New perspective on uncultured bacterial phylogenetic division OP11. Appl Environ Microbiol 70: 845-849
24. Harvey CF, Swartz CH, Badruzzaman ABM, Keon-Blute N, Yu W, Ali MA, Jay J, Beckie R, Niedan V, Brabander D, Oates PM, Ashfaque KN, Islam S, Hemond HF, Ahmed MF (2002) Arsenic mobility and groundwater extraction in Bangladesh. Science 298: 1602-1606
25. Henckel T, Friedrich M, Conrad R (1999) Molecular analyses of the methane-oxidizing microbial community in rice field soil by targeting the genes of the 16S rRNA, particulate methane monooxygenase, and methanol dehydrogenase. Appl Environ Microbiol 65: 1980-1990
26. Hering JG, Kneebone PE (2002) Biogeochemical controls on arsenic occurrence and mobility in water supplies. In: Frankenberger, WT (ed.) Environmental chemistry of arsenic. Marcel Dekker, New York, pp. 155-180
27. Hery M, van Dongen BE, Gill F, Mondal D, Vaughan DJ, Pancost RD, Polya DA, Lloyd JR (2010) Arsenic release and attenuation in low organic carbon aquifer sediments from West Bengal. Geobiology 8: 155-168
28. Hong S, Bunge J, Leslin C, Jeon S, Epstein SS (2009) Polymerase chain reaction primers miss half of rRNA microbial diversity. ISME Journal 3
29. Huber T, Faulkner G, Hugenholtz P (2004) Bellerophon: a program to detect chimeric sequences in multiple sequence alignments. Bioinformatics 20: 2317-2319
30. Hugenholtz P, Pitulle C, Hershberger KL, Pace NR (1998) Novel division level bacterial diversity in a Yellowstone hot spring. Journal of Bacteriology 180: 366-376
31. Islam FS, Gault AG, Boothman C, Polya DA, Charnock JM, Chatterjee D, Lloyd JR (2004) Role of metal-reducing bacteria in arsenic release from Bengal delta sediments. Nature 430: 68-71

32. Kalbitz K, Kaiser K (2008) Contribution of dissolved organic matter to carbon storage in forest mineral soils. Journal of Plant Nutrition and Soil Science-Zeitschrift Fur Pflanzenernahrung Und Bodenkunde 171: 52-60
33. Kappler A, Straub KL (2005) Geomicrobiological Cycling of Iron. Reviews in Mineralogy & Geochemistry 59: 85-108
34. Katsoyiannis IA, Zouboulis AI (2004) Application of biological processes for the removal of arsenic from groundwaters. Water Research 38: 17-26
35. Kennedy CB, Scott SD, Ferris FG (2003) Ultrastructure and potential sub-seafloor evidence of bacteriogenic iron oxides from axial volcano, Juan de Fuca Ridge, North-east Pacific Ocean. Fems Microbiology Ecology 43: 247-254
36. Kogel-Knabner I (2002) The macromolecular organic composition of plant and microbial residues as inputs to soil organic matter. Soil Biol Biochem 34: 139-162
37. Lane DJ (1991) 16S/23S rRNA sequencing. In: Stackebrandt, E, Goodfellow, M (eds.) Nucleic Acid Techniques in Bacterial Systematics. Wiley, New York, pp. 115-175
38. Lear G, Song B, Gault AG, Polya DA, Lloyd JR (2007) Molecular analysis of arsenate-reducing bacteria within Cambodian sediments following amendment with acetate. Appl Environ Microbiol 73: 1041-1048
39. Li H, Zhang Y, Li DS, Xu H, Chen GX, Zhang CG (2009) Comparisons of different hypervariable regions of rrs genes for fingerprinting of microbial communities in paddy soils. Soil Biol Biochem 41: 954-968
40. Lidstrom ME (2006) Aerobic methylotrophic prokaryotes. In: Dworkin, M, Falkow, S, Rosenberg, E, Schleifer, KH, Stackebrandt, E (eds.) The prokaryotes, vol. 1. Springer, New York, pp. 618-634
41. Liu D, Dong H, Bishop ME, Wang H, Agrawal A, Tritschler S, Eberl DD, Xie S (2011) Reduction of structural Fe(III) in nontronite by methanogen Methanosarcina barkeri. Geochimica et Cosmochimica Acta 75: 1057-1071
42. Lockhart PJ, Steel MA, Hendy MD, Penny D (1994) Recovering evolutionary trees under a more realistic model of sequence evolution. Molecular Biology and Evolution 11: 605-612
43. Luton PE, Wayne JM, Sharp RJ, Riley PW (2002) The mcrA gene as an alternative to 16S rRNA in the phylogenetic analysis of methanogen populations in landfill. Microbiology-Sgm 148: 3521-3530

44. Macur RE, Jackson CR, Botero LM, McDermott TR, Inskeep WP (2004) Bacterial populations associated with the oxidation and reduction of arsenic in an unsaturated soil. Environmental Science & Technology 38: 104-111
45. Meyer J, Michalke K, Kouril T, Hensel R (2008) Volatilisation of metals and metalloids: An inherent feature of methanoarchaea? Systematic and Applied Microbiology 31: 81-87
46. Mukhopadhyay R, Rosen BP, Pung LT, Silver S (2002) Microbial arsenic: from geocycles to genes and enzymes. Fems Microbiology Reviews 26: 311-325
47. Muyzer G, Dewaal EC, Uitterlinden AG (1993) Profiling of complex microbial-populations by denaturing gradient gel-electrophoresis analysis of polymerase chain reaction-amplified genes-coding for 16s ribosomal-RNA. Appl Environ Microbiol 59: 695-700
48. Neubauer SC, Emerson D, Megonigal JP (2002) Life at the energetic edge: Kinetics of circumneutral iron oxidation by lithotrophic iron-oxidizing bacteria isolated from the wetland-plant rhizosphere. Appl Environ Microbiol 68: 3988-3995
49. Neumann RB, Ashfaque KN, Badruzzaman ABM, Ali MA, Shoemaker JK, Harvey CF (2010) Anthropogenic influences on groundwater arsenic concentrations in Bangladesh. Nat Geosci 3: 46-52
50. Nicol GW, Glover LA, Prosser JI (2003) The impact of grassland management on archaeal community structure in upland pasture rhizosphere soil. Environmental Microbiology 5: 152-162
51. Ohno T, Zibilske LM (1991) Determination of low concentrations of phosphorus in soil extracts using malachite green. Soil Science Society of America Journal 55: 892-895
52. Ohnuki T, Sakamoto F, Kozai N, Ozaki T, Yoshida T, Narumi I, Wakai E, Sakai T, Francis AJ (2004) Mechanisms of arsenic immobilization in a biomat from mine discharge water. Chem Geol 212: 279-290
53. Oremland RS, Stolz JF (2003) The ecology of arsenic. Science 300: 939-944
54. Oremland RS, Stolz JF (2005) Arsenic, microbes and contaminated aquifers. Trends in Microbiology 13: 45-49
55. O'Sullivan LA, Webster G, Fry JC, Parkes RJ, Weightman AJ (2008) Modified linker-PCR primers facilitate complete sequencing of DGGE DNA fragments. Journal of Microbiological Methods 75: 579-581

56. Ovreas L, Forney L, Daae FL, Torsvik V (1997) Distribution of bacterioplankton in meromictic Lake Saelenvannet, as determined by denaturing gradient gel electrophoresis of PCR-amplified gene fragments coding for 16S rRNA. Appl Environ Microbiol 63: 3367-3373
57. Roberts LC, Hug SJ, Dittmar J, Voegelin A, Saha GC, Ali MA, Badruzzanian ABM, Kretzschniar R (2007) Spatial distribution and temporal variability of arsenic in irrigated rice fields in Bangladesh. 1. Irrigation water. Environmental Science & Technology 41: 5960-5966
58. Silver S, Phung LT (2005) A bacterial view of the periodic table: genes and proteins for toxic inorganic ions. Journal of Industrial Microbiology & Biotechnology 32: 587-605
59. Smedley PL, Kinniburgh DG (2002) A review of the source, behaviour and distribution of arsenic in natural waters. Appl Geochem 17: 517-568
60. Sobolev D, Roden EE (2002) Evidence for rapid microscale bacterial redox cycling of iron in circumneutral environments. Antonie Van Leeuwenhoek 81: 587-597
61. Steinberg LM, Regan JM (2008) Phylogenetic Comparison of the Methanogenic Communities from an Acidic, Oligotrophic Fen and an Anaerobic Digester Treating Municipal Wastewater Sludge. Appl Environ Microbiol 74: 6663-6671
62. Straub KL, Benz M, Schink B, Widdel F (1996) Anaerobic, nitrate-dependent microbial oxidation of ferrous iron. Appl Environ Microbiol 62: 1458-1460
63. Sultana M, Haertig C, Planer-Friedrich B, Seifert J, Schloemann M (2011) Bacterial Communities in Bangladesh Aquifers Differing in Aqueous Arsenic Concentration. Geomicrobiol J 28: 198-211
64. Sutton NB, van der Kraan GM, van Loosdrecht MCM, Muyzer G, Bruining J, Schotting RJ (2009) Characterization of geochemical constituents and bacterial populations associated with As mobilization in deep and shallow tube wells in Bangladesh. Water Research 43: 1720-1730
65. Tamura K, Dudley J, Nei M, Kumar S (2007) MEGA4: Molecular evolutionary genetics analysis (MEGA) software version 4.0. Molecular Biology and Evolution 24: 1596-1599
66. Thompson JD, Gibson TJ, Plewniak F, Jeanmougin F, Higgins DG (1997) The CLUSTAL_X windows interface: flexible strategies for multiple sequence alignment aided by quality analysis tools. Nucleic Acids Research 25: 4876-4882

67. Violante A, Del Gaudio S, Pigna M, Ricciardella M, Banerjee D (2007) Coprecipitation of arsenate with metal oxides. 2. Nature, mineralogy, and reactivity of iron(III) precipitates. Environmental Science & Technology 41: 8275-8280
68. Violante A, Krishnamurti GSR-, Huang PM (2002) Impact of organic substances on the formation and trasformation of metal oxides in soil environments. In: Huang, PM, Bollag, JM, Senesi, N (eds.) Interactions between soil particles and microorganisms. John Wiley & Sons, Chichester, UK, pp. 133-171
69. Wagner M, Roger AJ, Flax JL, Brusseau GA, Stahl DA (1998) Phylogeny of dissimilatory sulfite reductases supports an early origin of sulfate respiration. Journal of Bacteriology 180: 2975-2982
70. Wang JJ, Muyzer G, Bodelier PLE, Laanbroek HJ (2009) Diversity of iron oxidizers in wetland soils revealed by novel 16S rRNA primers targeting Gallionella-related bacteria. Isme Journal 3: 715-725
71. Webster G, Newberry CJ, Fry JC, Weightman AJ (2003) Assessment of bacterial community structure in the deep sub-seafloor biosphere by 16S rDNA-based techniques: a cautionary tale. Journal of Microbiological Methods 55: 155-164
72. Webster G, Parkes RJ, Cragg BA, Newberry CJ, Weightman AJ, Fry JC (2006) Prokaryotic community composition and biogeochemical processes in deep subseafloor sediments from the Peru Margin. Fems Microbiology Ecology 58: 65-85
73. Webster G, Sass H, Cragg BA, Gorra R, Knab NJ, Green CJ, Mathes F, Fry JC, Weightman AJ, Parkes RJ (2011) Enrichment and cultivation of prokaryotes associated with the sulphate-methane transition zone of diffusion-controlled sediments of Aarhus Bay, Denmark, under heterotrophic conditions. Fems Microbiology Ecology 77: 248-263
74. Webster G, Yarram L, Freese E, Koester J, Sass H, Parkes RJ, Weightman AJ (2007) Distribution of candidate division JS1 and other Bacteria in tidal sediments of the German Wadden Sea using targeted 16S rRNA gene PCR-DGGE. Fems Microbiology Ecology 62: 78-89
75. Wu ZJ, Yuan LX, Jia N, Wang YH, Sun LG (2009) Microbial biomineralization of iron seepage water: Implication for the iron ores formation in intertidal zone of Zhoushan Archipelago, East China Sea. Geochemical Journal 43: 167-177
76. Zhou JZ, Bruns MA, Tiedje JM (1996) DNA recovery from soils of diverse composition. Appl Environ Microbiol 62: 316-322

Figure Legends

Figure 1.

FT-IR (A) and liquid-state ^{13}C NMR spectra (B) of the extracted organic material present in the Fe-As co-precipitation products. The main functional groups composing the organic material have been reported in both spectra.

Figure 2.

(A) SEM of Fe-As co-precipitation products showing abundant bacterial stalks, morphologically analogous to *Gallionella*. (B) SEM magnification of *Gallionella*-like stalks. White arrows indicate nucleation of iron oxides on *Gallionella*-like stalks.

Figure 3.

(A) *Bacteria* and (B) *Archaea* 16S rRNA gene targeted PCR-DGGE analysis of Fe-As co-precipitation products. Lanes represent different sampling years from 2005 to 2009; lanes marked M, DGGE marker [71]. Numbered bands were excised and sequenced (Tables 4 and 5).

Figure 4.

Taxonomic affiliation of bacterial 16S rRNA genes recovered from Fe-As co-precipitation products sampled in 2008.

Figure 5.

Phylogenetic tree showing the relationship of the *Proteobacteria* 16S rRNA gene sequences in the bacterial clone library from the Fe-As co-precipitation products sampled in 2008 to their nearest environmental and pure culture sequences. The tree was obtained using Minimum Evolution and LogDet distance with 850 bases of aligned 16S rRNA gene sequences and rooted with representative sequences of the *Alphaproteobacteria*; *Anaplasma marginale* (CP001079), *Rhizobium etli* (CP001074) and *Hirschia baltica* (CP001678). Bootstrap support values over 50% (1000 replicates) are shown. Sequences retrieved in this study are in bold.

Figure 6.

(A) *Gallionella* 16S rRNA gene, (B) methanogen 16S rRNA gene, and (C) *dsrB* gene targeted PCR-DGGE analysis of Fe-As co-precipitation products. Lanes represent sampling

years from 2005 to 2009; lanes marked M, DGGE marker [71]. Numbered bands were excised and sequenced (Table 5).

Supplementary Figure S1

PCR-DGGE (A) and cluster analysis (B) of bacterial 16S rRNA gene profiles of Fe-As co-precipitation products from a water storage tank in Bangladesh. Lanes represent different sampling years from 2005 to 2009; lanes marked M, DGGE marker [71].

Supplementary Figure S2

PCR-DGGE (A) and cluster analysis (B) of archaeal 16S rRNA gene profiles of Fe-As co-precipitation products from a water storage tank in Bangladesh. Lanes represent different sampling years from 2005 to 2009; lanes marked M, DGGE marker [71].

Figures

Figure 1

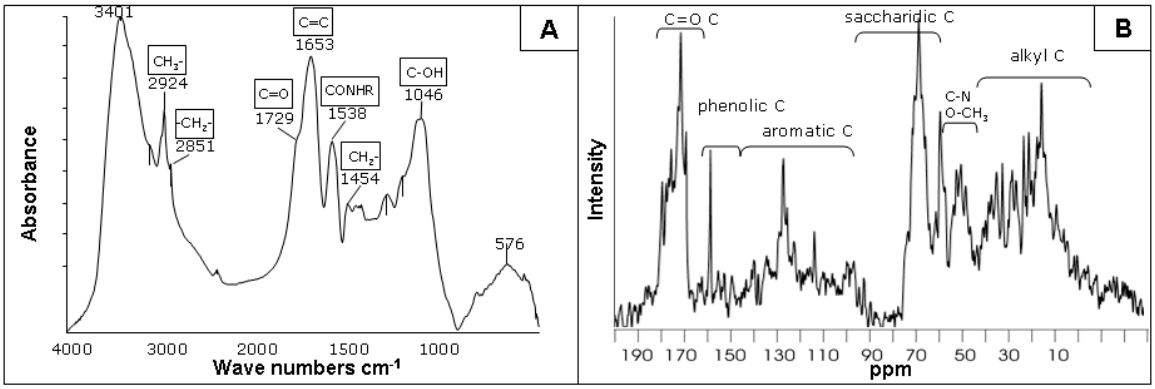

Figure 2

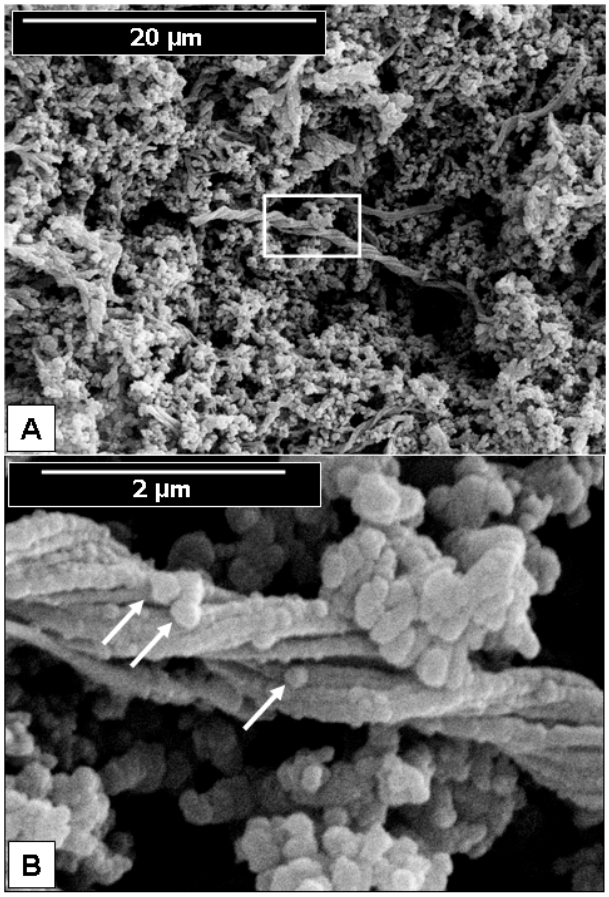

Figure 3

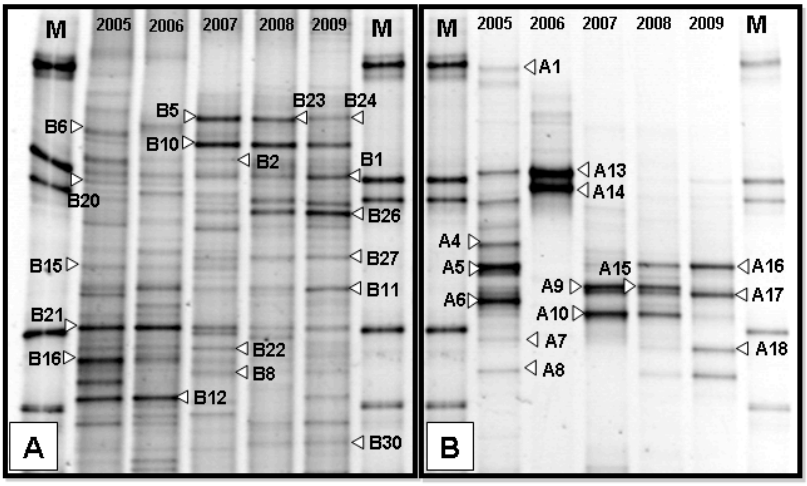
M
2005
2006
2007
2008
2009
M
B6
B20
B15
B21
B16
B5
B10
B12
B23
B24
B2
B1
B26
B27
B11
B22
B8
B30
A
M
2005
2006
2007
2008
2009
M
A1
A13
A14
A4
A5
A6
A9
A10
A7
A8
A15
A16
A17
A18
B

Figure 4

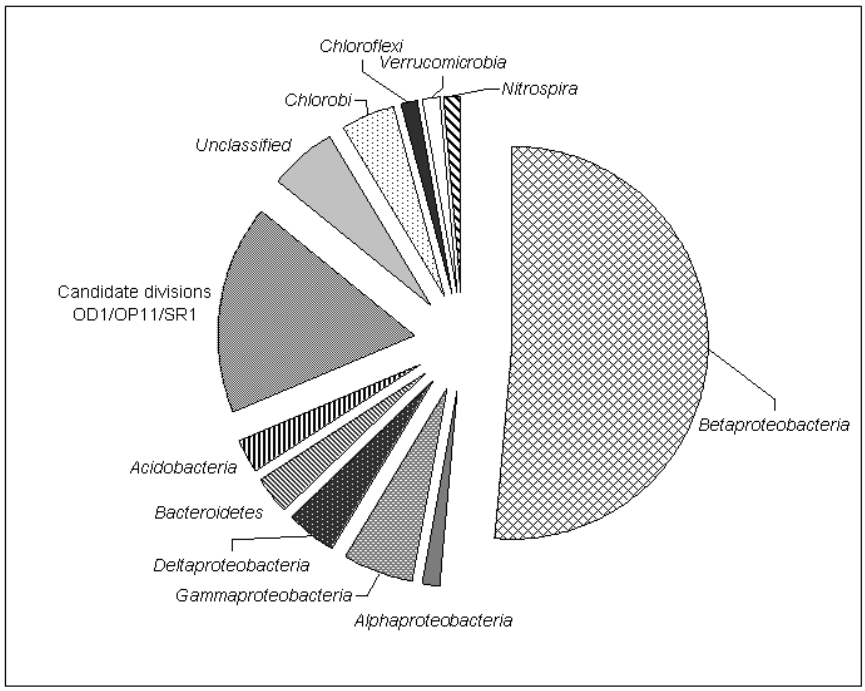
Chloroflexi
Verrucomicrobia
Nitrospira
Chlorobi
Unclassified
Candidate divisions
OD1/OP11/SR1
Betaproteobacteria
Acidobacteria
Bacteroidetes
Deltaproteobacteria
Gammaproteobacteria
Alphaproteobacteria

Figure 5

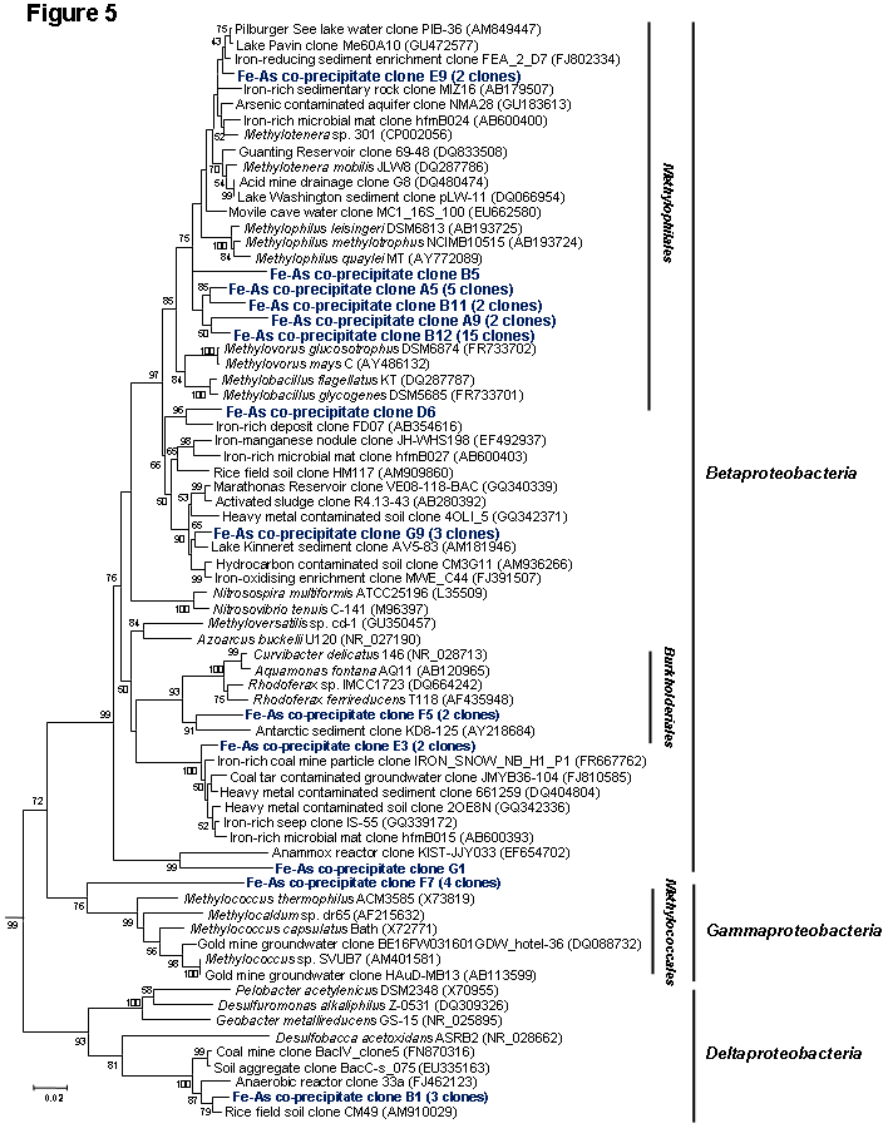
Pilburger See lake water clone PIB-36 (AM849447)
Lake Pavin clone Me60A10 (GU472577)
Iron-reducing sediment enrichment clone FEA_2_D7 (FJ802334)
Fe-As co-precipitate clone E9 (2 clones)
Iron-rich sedimentary rock clone MIZ16 (AB179507)
Arsenic contaminated aquifer clone NMA28 (GU183613)
Iron-rich microbial mat clone hfmB024 (AB600400)
Methylotenera sp. 301 (CP002056)
Guanting Reservoir clone 69-48 (DQ833508)
Methylotenera mobilis JLW8 (DQ287786)
Acid mine drainage clone G8 (DQ480474)
Lake Washington sediment clone pLW-11 (DQ066954)
Movile cave water clone MC1_16S_100 (EU662580)
Methylophilus leisingeri DSM6813 (AB193725)
Methylophilus methylotrophus NCIMB10515 (AB193724)
Methylophilus quaylei MT (AY772089)
Fe-As co-precipitate clone B5
Fe-As co-precipitate clone A5 (5 clones)
Fe-As co-precipitate clone B11 (2 clones)
Fe-As co-precipitate clone A9 (2 clones)
Fe-As co-precipitate clone B12 (15 clones)
Methylovorus glucosotrophus DSM6874 (FR733702)
Methylovorus mays C (AY486132)
Methylobacillus flagellatus KT (DQ287787)
Methylobacillus glycogenes DSM5685 (FR733701)
Fe-As co-precipitate clone D6
Iron-rich deposit clone FD07 (AB354616)
Iron-manganese nodule clone JH-WHS198 (EF492937)
Iron-rich microbial mat clone hfmB027 (AB600403)
Rice field soil clone HM117 (AM909860)
Marathonas Reservoir clone VE08-118-BAC (GQ340339)
Activated sludge clone R4.13-43 (AB280392)
Heavy metal contaminated soil clone 4OLI_5 (GQ342371)
Fe-As co-precipitate clone G9 (3 clones)
Lake Kinneret sediment clone AVS-83 (AM181946)
Hydrocarbon contaminated soil clone CM3G11 (AM936266)
Iron-oxidising enrichment clone MWE_C44 (FJ391507)
Nitrosospira multiformis ATCC25196 (L35509)
Nitrosovibrio tenuis C-141 (M96397)
Methyloversatilis sp. cd-1 (GU350457)
Azoarcus buckelii U120 (NR_027190)
Curvibacter delicatus 146 (NR_028713)
Aquamonas fontana AQ11 (AB120965)
Rhodoferax sp. IMCC1723 (DQ664242)
Rhodoferax fermireducens T118 (AF435948)
Fe-As co-precipitate clone F5 (2 clones)
Antarctic sediment clone KD8-125 (AY218684)
Fe-As co-precipitate clone E3 (2 clones)
Iron-rich coal mine particle clone IRON_SNOW_NB_H1_P1 (FR667762)
Coal tar contaminated groundwater clone JMYB36-104 (FJ810585)
Heavy metal contaminated sediment clone 661259 (DQ404804)
Heavy metal contaminated soil clone 2OE8N (GQ342336)
Iron-rich seep clone IS-55 (GQ339172)
Iron-rich microbial mat clone hfmB015 (AB600393)
Anammox reactor clone KIST-JJY033 (EF654702)
Fe-As co-precipitate clone G1
Fe-As co-precipitate clone F7 (4 clones)
Methylococcus thermophilus ACM3585 (X73819)
Methylocaldum sp. dr65 (AF215632)
Methylococcus capsulatus Bath (X72771)
Gold mine groundwater clone BE16FW031601GDW_hotel-36 (DQ088732)
Methylococcus sp. SVUB7 (AM401581)
Gold mine groundwater clone HAuD-MB13 (AB113599)
Pelobacter acetylenicus DSM2348 (X70955)
Desulfuromonas alkaliphilus Z-0531 (DQ309326)
Geobacter metallireducens GS-15 (NR_025895)
Desulfobacca acetoxidans ASRB2 (NR_028662)
Coal mine clone BacIV_clone5 (FN870316)
Soil aggregate clone BacC-s_075 (EU335163)
Anaerobic reactor clone 33a (FJ462123)
Fe-As co-precipitate clone B1 (3 clones)
Rice field soil clone CM49 (AM910029)
0.02
Methylophilales
Betaproteobacteria
Burkholderiales
Methylococcales
Gammaproteobacteria
Deltaproteobacteria

Figure 6

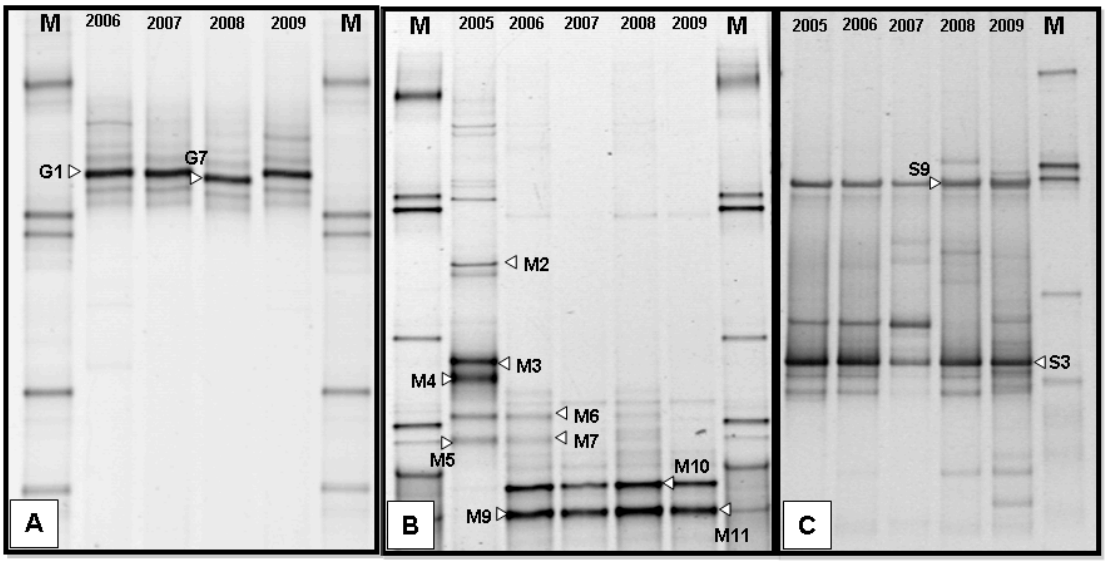
M
2006
2007
2008
2009
M
G1
G7
A
M
2005
2006
2007
2008
2009
M
M2
M3
M4
M5
M6
M7
M9
M10
M11
B
2005
2006
2007
2008
2009
M
S9
S3
C

Supplementary Figure S1

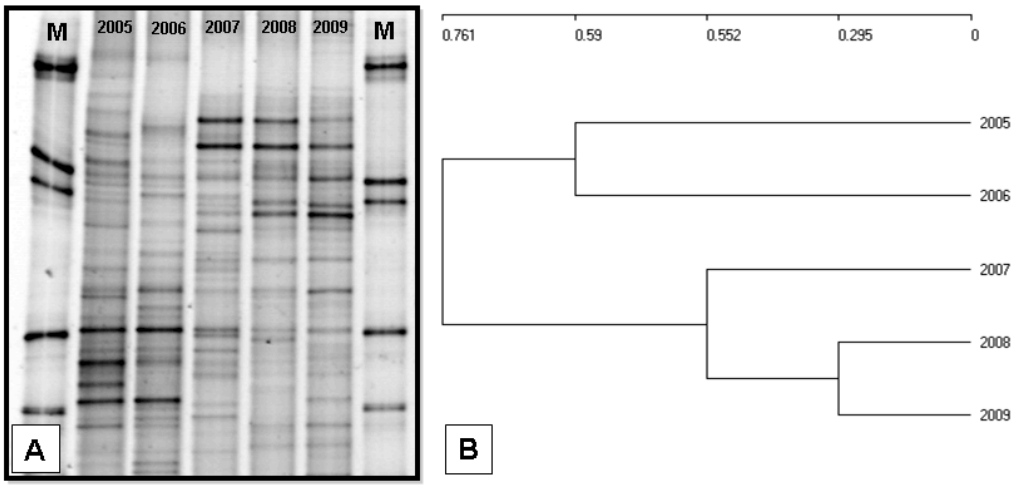

Supplementary Figure S2